Surface & Coatings Technology 204 (2009) 256–262

Contents lists available at ScienceDirect

Surface & Coatings Technology

journal homepage: www.elsevier.com/locate/surfcoat

# Oxidation post-treatment of hard AlTiN coating for machining of hardened steels

J.L. Endrino [a,*], G.S. Fox-Rabinovich [b], R. Escobar Galindo [a,c], W. Kalss [d], S. Veldhuis [b], L. Soriano [e], J. Andersson [f], A. Gutiérrez [e]

[a] Instituto de Ciencia de Materiales de Madrid, E-28049 Madrid, Spain
[b] McMaster University, Ontario, Canada L8S 4 L7
[c] Centro de Micro-Análisis de Materiales, Universidad Autónoma de Madrid, E-28049 Madrid, Spain
[d] OC Oerlikon Balzers AG, Li-9496 Balzers, Liechtenstein
[e] Departamento de Física Aplicada and Instituto Nicolás Cabrera, Universidad Autónoma de Madrid, E-28049 Madrid, Spain
[f] The Angstrom Laboratory, Uppsala University, Uppsala, Sweden

ARTICLE INFO

*Article history:*
Received 12 January 2009
Accepted in revised form 9 July 2009
Available online 17 July 2009

*Keywords:*
PVD
Nano-composite structure
Cutting tools life
High performance machining
RBS
XANES

ABSTRACT

In this study, cemented carbide ball nose end mills with nano-crystalline $Al_{0.67}Ti_{0.33}N$ hard PVD coatings deposited by cathodic arc evaporation were annealed at 700 °C during 2 h in a controlled atmosphere environment (argon + oxygen mixture) and in vacuum. The changes of structure and properties of the treated coating surfaces have been analyzed using both cross-sectional scanning electron microscopy (SEM) and x-ray absorption spectroscopy (XAS) of the N–K and O–K edges. Cutting tools have been run through ball nose end milling of hardened H13 steel (HRC 50) where temperature or stress dominating phenomena control tool life. The data obtained indicate that an AlTiN coated cutting tool can be modified upon annealing at low temperature conditions and should be considered as a composite surface engineered material. It is shown that increased tool life could be achieved if annealing of AlTiN is performed in an oxygen-containing atmosphere. A variety of different characteristics should be optimized to achieve better wear resistance of the cutting tools with annealed $Al_{0.67}Ti_{0.33}N$ coating under high temperature and stress cutting conditions.

© 2009 Elsevier B.V. All rights reserved.

## 1. Introduction

Maximum wear resistance of coated cutting tools should be expected from the coating that possesses a favorable combination of hardness, toughness and low friction [1]. Development of ceramic coatings with sufficiently high hardness (above 20–25 GPa), improved toughness and low friction is a challenge [2]. This could be done in a number of ways, in particular by post-treatment of hard coatings. Coated cemented carbide inserts could be considered as a composite material that consists of a WC/Co substrate with an AlTiN hard coating. Tool life and wear performance of this material depends both on properties of the coating and substrate material as well.

Al-rich TiAlN coatings are widely used for high performance machining applications [3–8]. It is known that annealing of the AlTiN coating could result in hardness improvements at elevated temperatures [9,10]. During annealing, a beneficial nano-composite structure of the coating is formed that includes the formation of nano-scale sized domains of c-AlN in a c-(Ti,Al)N matrix [2,3]. The authors of this manuscript have published elsewhere a very detail HRTEM study on the thermal evolution of such an Al-rich AlTiN coating [9]. It was shown elsewhere that annealing of AlTiN coating in vacuum at elevated temperatures (900 °C and above) results in significant tool life improvement under conditions of high-speed turning of annealed 1040 steel [9,10]. This takes place due to formation of the nano-composite structure of the coating that leads to micro-hardness increase and reduction of density of lattice imperfections with temperature [10]. There is some additional information in literature on beneficial impact of annealing on the coated cutting tool life [3,11,12]. However, the shortcoming of these post-treatments is the reduction of plastic properties and embrittlement of the interface between the coating and the cemented carbide substrate that could become a problem in operations such as interrupted cutting. The coating toughness and the formation of tribofilms are as important, if not more, as hardness [13,14]. That is why in this paper annealing is performed at lower temperatures, in order to optimize plastic properties of the coating after the post-treatment and avoid catastrophic failure by delamination. Formation of the protective films on the friction surface is known to be very beneficial from the point of view of the wear resistance improvements [15]. However, there is a lack of information on the impact of wear performance characteristics of the tool surface of cutting tools with Al-rich TiAlN coatings for hard machining operations after annealing in an oxidative atmosphere.

The goal of this paper is twofold: (1) to investigate the impact of annealing of the nano-crystalline AlTiN coating in an oxidative atmosphere composed of argon and oxygen mixture on coated tool life and wear behavior in hard machining; (2) to make a detailed characterization study using RBS and XAS of the top oxidized surface layer in the $Al_{67}Ti_{33}N$ film after annealing in $Ar + O_2$ atmosphere.

* Corresponding author. Tel.: +34 91 334 9000x102; fax: +91 372 0623.
*E-mail address:* jlendrino@icmm.csic.es (J.L. Endrino).

0257-8972/$ – see front matter © 2009 Elsevier B.V. All rights reserved.
doi:10.1016/j.surfcoat.2009.07.010

## 2. Experimental

The AlTiN hard coatings investigated were synthesized using a Balzers' Rapid Coating System (RCS) deposition machine in a cathodic arc ion plating mode. Mirror polished cemented carbide WC/Co turning insert substrates were used for the coating deposition. The deposition times were adjusted in order to achieve the thickness of all the coatings within $3.5 \pm 0.2$ μm. The temperature of the substrates during deposition was held at approximately 600 °C.

Annealing of the coated tools was performed in high vacuum at $1 \times 10^{-6}$ mbar and in an argon and oxygen mixture (80/20 ratio) at 700 ºC for a duration of 2 h. EDX analysis was used to study elemental composition of the cross-sections of AlTiN coated cemented carbide inserts after annealing at various temperatures and investigate the critical temperature for diffusion of Co.

A Siemens D5000 diffractometer (radiation wavelength CuKα = 1.5406 Å) was used to perform XRD analysis and identify the phases formed.

RBS experiments were performed with the 5 MV HVEE Tandetron accelerator situated at the Centro de Micro-Análisis de Materiales at Universidad Autónoma de Madrid [16]. RBS spectra were collected using a 2 MeV $He^+$ beam. Besides, in order to improve the sensitivity to oxygen, experiments at the 3.035 MeV non-Rutherford cross section resonance $^{16}O(\alpha,\alpha)^{16}O$ were performed. Experiments near the resonance were performed at energies of 3.028, 3.055 and 3.072 MeV to determine the oxygen content profile. The data was acquired simultaneously with two silicon surface barrier detectors located at scattering angles of 170° with an energy resolution of 16 keV and an ion dose of 5 μC per detector. The experimental spectra were fitted using the programs RBX and SIMRA [17,18].

X-ray absorption spectroscopy (XAS) at the N–K and O–K edges of the treated samples was studied at beamline 7.0 of the Advanced Light Source (ALS) at Lawrence Berkeley National Laboratory. The experiments were performed by measuring simultaneously the total electron (TEY) and total fluorescence (TFY) yields.

The cutting tests were performed under conditions shown in Table 1.

Scanning electron microscope (SEM) was used to study morphology of the worn tools and the chips cross sections.

## 3. Results and discussion

### 3.1. Selection of post-treatment conditions of coated AlTiN tools

Previous cutting tool life studies have shown that annealing above 800 °C under conditions of continuous high-speed turning of the annealed structural steel 1040 can be favorable [3,9,10]. This is because the temperature at the tool/workpiece interface was high and the stresses are relatively low. However, under interrupted cutting conditions, such as ball nose end milling, the stress induced by the load-cycling conditions are dominating on the tool/workpiece interface and there is a higher risk of catastrophic failure when the annealing is done at elevated temperatures (above 700–800 °C) since the coating/substrate interface starts to play a dominant role.

**Table 1**
Cutting data for the experiments performed.

| | |
|---|---|
| Machining operation | Ball nose end milling |
| Cutting tool substrates | CC ball nose end mills, $D = 19$ mm |
| Workpiece material | H13 steel |
| Hardness | HRC 50 |
| Speed (m/min) | 200 (7000 rpm) |
| Feed rate | 840 mm/min |
| Axial depth of cut | 5 mm |
| Radial depth of cut | 1 mm |

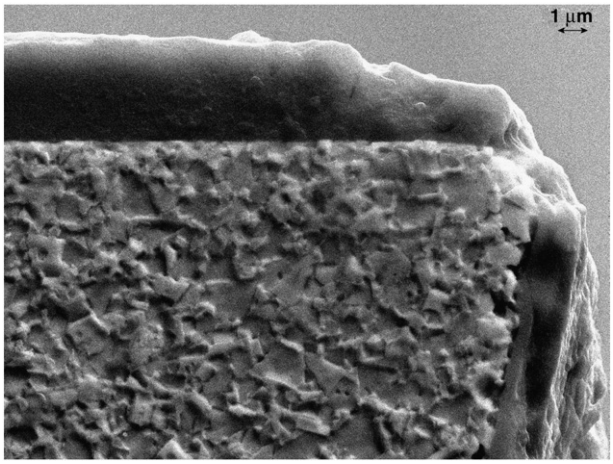


**Fig. 1.** SEM micrograph of the cross section of $Al_{67}Ti_{33}N$ coating deposited onto a cemented carbide insert.

A cross-section of an AlTiN coated insert is presented in Fig. 1. The AlTiN film coats both sides of the tool, however, it is thinner close to the edge due to ion plating (i.e. high substrate bias) effects in the edge region. EDX data (Table 2) was collected at the coating layer, at the interface between the coating and the cemented carbide substrate and at the core of the cemented carbide tool for various annealing temperatures. The collected EDX data indicates that at temperatures above 700 ºC, the Co binder segregates at the coating/substrate interface and further diffuses into the coating layer. The segregation of large amounts of Co to the interface probably suggests formation of the η-phase at the cemented substrate [19], which would likely result in a decrease in tool life of AlTiN coated end mill cutters annealed at temperatures above 700 °C.

In contrast, tool life improvement could be achieved by the formation of surface tribofilm by performing the annealing treatment in an oxygen-containing atmosphere. It is known from literature that oxygen-containing but nitrogen-free atmosphere enhances formation of protective alumina films of the surface and improve oxidation stability of TiAl-based alloys [20–23]. That is why the annealing of the ball nose end mills with AlTiN coating was also performed in $Ar + O_2$ (80/20 at.% ratio) atmosphere.

### 3.2. Characterization of nano-crystalline $Al_{67}Ti_{33}N$ film annealed in $Ar + O_2$ atmosphere

Fig. 2a shows the RBS collected spectra at the 3.035 MeV oxygen resonance for the oxidized sample at 700 °C in $O_2 + Ar$ environment. The RBS experimental data (open circles) and the global fitting of results have been shifted vertically from the contributions of the elemental spectra (lower part of the graphs) in Fig. 1 for clarity purposes. The fitting of the results using SIMNRA gave a very good

**Table 2**
EDX data on enrichment by Co of AlTiN coating/CC substrate interface vs. temperature of annealing.

| Temperature of annealing, °C | Co content, at.% | | | Enrichment of the AlTiN coating/CC substrate interface by cobalt, % to core material |
|---|---|---|---|---|
| | Coating layer | AlTiN coating/CC substrate interface | CC core | |
| As-deposited, 600 | Traces, below 0.2 | 8.7 | 7.6 | 13 |
| 700 | Traces, below 0.2 | 9.4 | 8.3 | 13 |
| 800 | 0.2 | 9.6 | 8.1 | 19 |
| 900 | 0.2 | 10.5 | 8.4 | 24 |

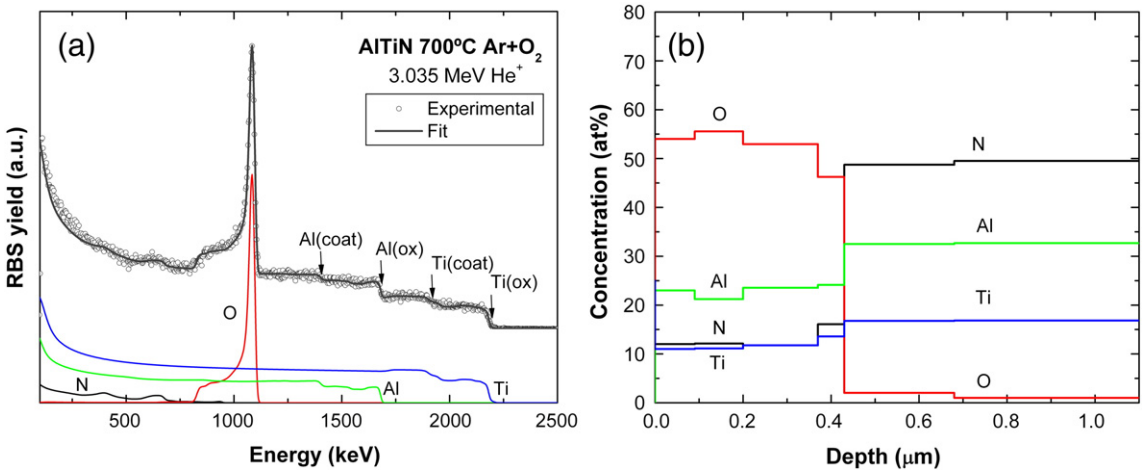


**Fig. 2.** RBS collected spectra at the 3.035 MeV oxygen resonance for the oxidized sample at 700 °C in $O_2$ + Ar environment. (a) RBS experimental data (open circles) and the global fitting of results have been shifted vertically from the contributions of the elemental spectra (lower part of the graphs) for clarity purposes. (b) Composition profiles obtained by RBX.

agreement with the experimental data. The presence of a clear oxygen resonance shows the benefit of using this non-RBS cross section in the quantitative analysis of oxide layers. The oxygen content was found to be 54 ± 1 at.% and kept practically constant through the oxide film (see composition profiles obtained by RBX in Fig. 2b). The experiments performed at energies close to the resonance confirm the homogeneous oxygen profile in the surface oxide layer. The oxide is formed by both aluminum and titanium compounds as both elements were detected at the surface of the sample at energies of 1685 and 2180 keV, respectively (see Fig. 1). This coexistence of both Ti and Al oxides at the surface has been reported in previous work on high temperature oxidized TiAl alloys using RBS to carry out a depth profile [22]. The oxide is richer in aluminum than titanium with an Al/Ti ratio of 2.0 ± 0.1, similar to the metal ratio in the AlTiN coating (see Fig. 2). The ratio O/Me in the oxide is 2.4 ± 0.2 for aluminum and 4.8 ± 0.2 for titanium. Therefore it is plausible that the oxide is formed by $TiO_2$ (rutile) + $Al_2O_3$ (alumina). A small but not negligible content of 10 at.% nitrogen was present in the oxide. The step observed in the titanium and aluminum RBS spectra revealed the presence of the AlTiN coating under the oxide layer. The composition of the nitride was found to be 50 ± 1 at.% nitrogen, 33 ± 1 at.% aluminum, 17 ± 1 at.% titanium. The oxygen content in the nitride coating was found to be less than 1 at.%.

Fig. 3 shows a cross-sectional SEM micrograph of the AlTiN sample with a top amorphous oxide layer, about half a micrometer in thickness, which was formed during the oxidation post-treatment. GIXRD patterns for the oxidized and as-deposited nano-crystalline $Al_{67}Ti_{33}N$ film are shown in Fig. 4. Both patterns show the presence of WC/Co substrate peaks, although these peaks are attenuated in the oxidized sample due to the increase in thickness after the oxidation post-treatment. Both the as-deposited film and the sample oxidized in oxygen and argon atmosphere show a (200) oriented fcc-TiAlN phase with a slight contribution of hcp-TiAlN as observed from the peak at 2-theta ~ 33°. The comparison of these two spectra confirms the amorphous character of the top oxide layer.

Fig. 5 shows x-ray absorption spectra at the N–K edge of as-deposited and annealed AlTiN samples, both in TEY and TFY mode. The bottom spectrum in Fig. 5a corresponds to the as-deposited sample measured in TEY mode, and is compatible with what can be expected for AlTiN compounds. The first region, between 395 eV and 402 eV, can be assigned to transitions between N-1s states and N-2p empty states hybridized with Ti-3d states. Two peaks are expected in this region due to the Ti-3d splitting into $e_g$ and $t_{2g}$ states [24,25]. On the other hand, the region at higher energies, between 402 eV and 410 eV, corresponds to N-2p states hybridized with Ti 4sp states and Al 3sp states.

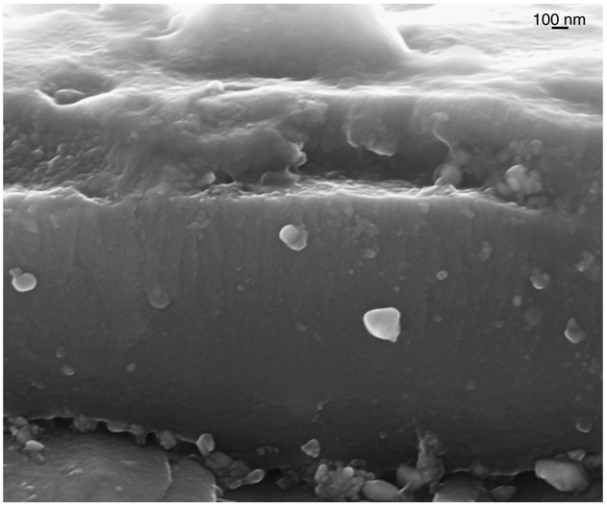


**Fig. 3.** Cross-sectional SEM image of the AlTiN coated WC/Co insert after annealing in $O_2$ + Ar environment at 700 °C during 1 h.

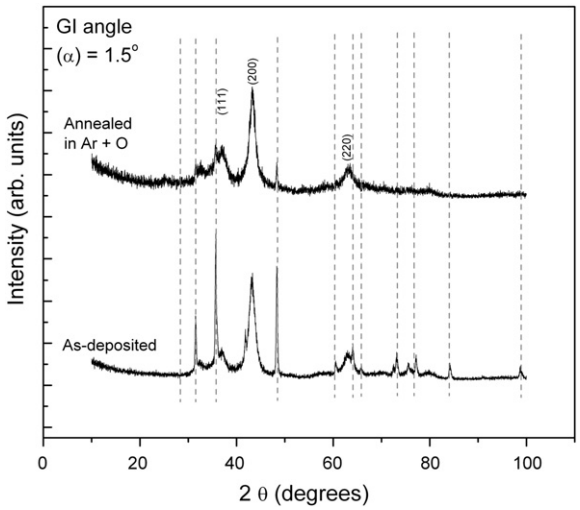


**Fig. 4.** Glancing incidence X-ray diffraction (GIXRD) pattern of as-deposited and oxidized AlTiN samples (dashed lines correspond to WC/Co substrate peaks).

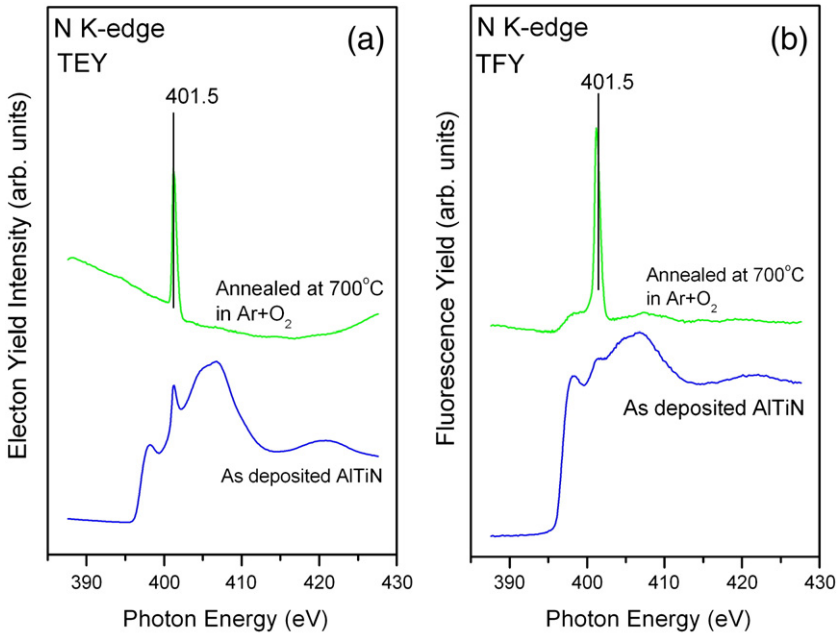


**Fig. 5.** N K-edge X-ray absorption spectra for oxidized and as-deposited and oxidized $Al_{67}Ti_{33}N$ film in (a) total electron yield (TEY) and (b) total fluorescence yield (TFY) mode.

The spectral lineshape of the sample measured in TFY mode is somewhat different due to self-absorption effects, but the observed features can be explained with the same assignments as the TEY spectrum.

For the annealed sample the XAS spectra radically change, presenting a single peak in TEY mode and a huge, sharp peak contained in a much lower plateau in TFY mode. Such a sharp peak at this position can only be assigned to molecular nitrogen. Similar behavior has already been observed in the oxidation process of a TiN thin film [25,26]. In this case, this would indicate that upon oxidation of the AlTiN film, nitrogen atoms are displaced by oxygen atoms so that they remain embedded as an impurity, but without chemically reacting. The small plateau detected in the FY mode indicates that there is a small proportion of the film, far away from the surface, that still remains as a nitride.

Fig. 6a shows x-ray absorption spectra at the O–K edge of the annealed AlTiN sample in TEY mode, together with a spectrum of amorphous $Al_2O_3$ and of $TiO_2$ in its rutile form for comparison. From a direct visual inspection, it seems clear that the result of the oxidation treatment consists mainly of a mixture of $Al_2O_3$ and $TiO_2$. To get some further information, we have tried to simulate the spectrum of the annealed sample as a sum of those of rutile and alumina, with their corresponding weights. This strategy has been previously used when studying Ti–Al oxides [27]. The result of the best fit, which is 40% rutile and 60% alumina is shown in Fig. 6b. Due to the small misfit between the spectrum of the annealed sample and the sum of rutile and

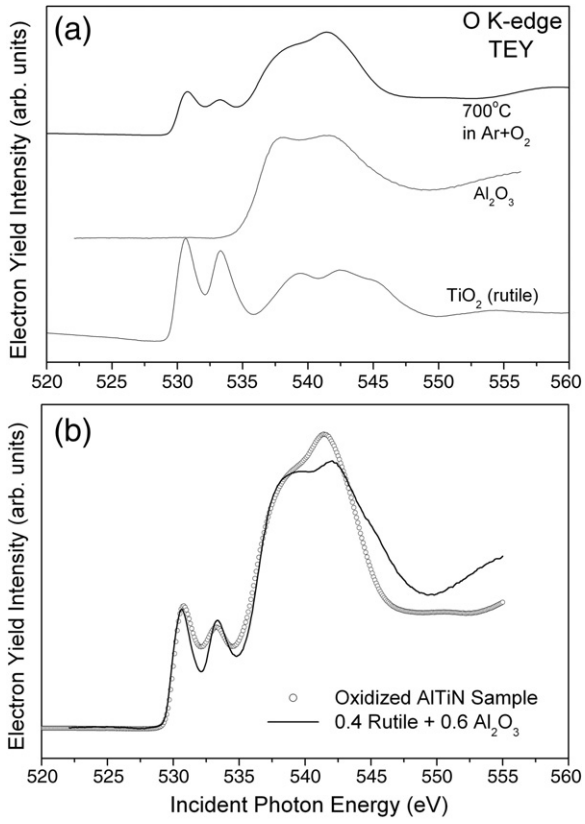


**Fig. 6.** (a) O K-edge X-ray absorption spectra of oxidized AlTiN coating in $O_2 + Ar$ environment and (b) comparison of sum of 40% rutile $TiO_2$ and 60% alumina with measured O–K spectra for AlTiN coating.

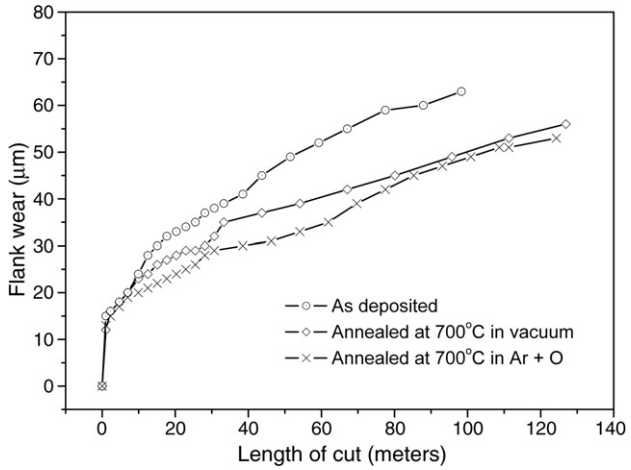


**Fig. 7.** Tool flank wear of the ballnose end mills with as-deposited AlTiN, vacuum annealed AlTiN and oxidized AlTiN films.

alumina spectra, especially at the valley between the $e_g$ and $t_{2g}$ states, and at the shoulder at 542 eV, we cannot exclude that there is some small amount of ternary Al–Ti–O compounds, or even Al–Ti–O–N compounds, but their relative weight should be low. The presence of an $Al_2O_3$ rich top-layer in the ball nose end milling cutters may be beneficial in machining experiments.

### 3.3. Cutting tests

Cutting experiments performed (Fig. 7) confirm the hypothesis that annealing in an oxygen-containing atmosphere can be beneficial. The cutting tool data shows that the tool life of the ball nose end mills annealed in an $Ar + O_2$ atmosphere is higher as compared to the tools without annealing and to the annealing done in vacuum.

The shapes of the chips and their surface morphologies during ball nose end milling are shown in Fig. 8. The chips from the end mill with AlTiN coating without annealing are relatively dull and have a large curl diameter (Fig. 8b). The annealing of the AlTiN coatings was found to change the microstructure of the chips (Fig. 8a). The chips that are generated on the surface of the end milling cutters with the AlTiN are forming at higher temperature at the interface. As a result, a $\gamma \rightarrow \alpha$ phase transformation that is taking place during cooling of the high-alloyed H 13 steel in air result in crack formation within a volume of the chips due to the brittleness of the formed martensite structure (cracks are indicated in the structure of the chips cross-section, see Fig. 8a). In contrast, the chips from the cutter with the AlTiN coatings after annealing in the oxygen-containing atmosphere are more intensively curled into a spiral (Fig. 8d,f) and show no formation of micro cracks (Fig. 8c,e). When a chip is sliding along the rake surface

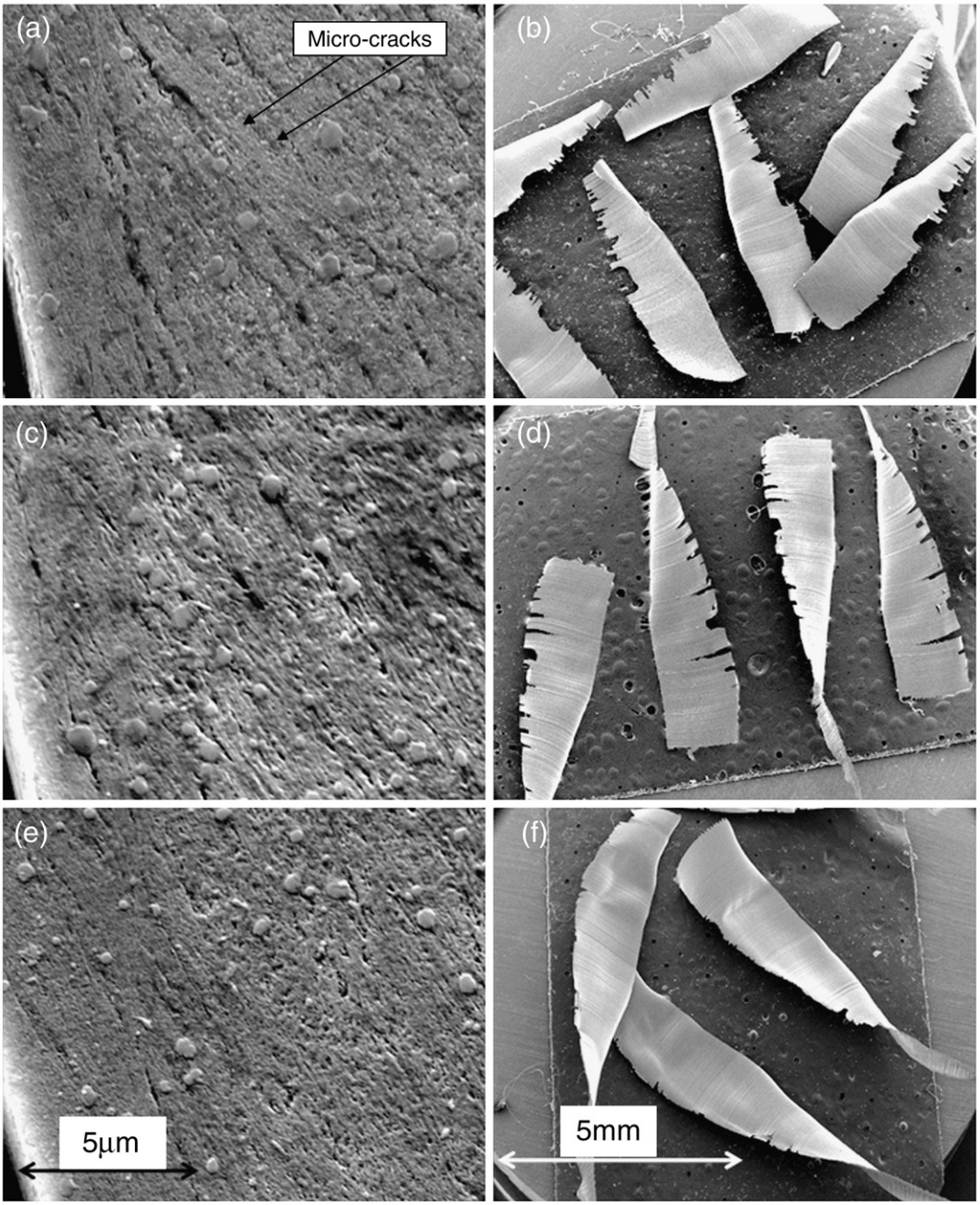


**Fig. 8.** Chips morphology of H13 steel chips collected during the running-in-stage: (a)–(b) as-deposited $Al_{67}Ti_{33}N$ film; (b)–(c) $Al_{67}Ti_{33}N$ film vacuum annealed at 700 °C; (d)–(e) $Al_{67}Ti_{33}N$ film oxidized at 700 °C.

of the end mill the curved flow lines are formed due to friction. An extended deformation zone could be observed close to the contact area of the chip. The SEM metallographic data obtained indicate that the actual tribological characteristics at the tool/chip interface have been improved by the post-treatments.

Surface morphology of the worn end mills with AlTiN coating with and without annealing is shown in Fig. 9. The data presented shows that pick up of the workpiece material (steel H 13) is taking place on both the rake and face surfaces of the cutting tools but the seizure intensity is much higher at the rake face. The seizure intensity drops for the annealed AlTiN coatings compared to the as-deposited state (Fig. 9a–b and c–f). This is especially clear for the rake worn faces (Fig. 9b–d–f). The lowest seizure intensity is observed on the rake surface of the ball nose end mills with AlTiN coating after annealing in the oxygen-containing atmosphere due to the alumina films formation. A smaller sticking zone is found on the surface of the ball nose end mills with AlTiN coating after annealing in the oxygen-containing atmosphere (Fig. 9e–f). The smaller size of the sticking zone is caused by the formation of the protective alumina films with high thermodynamic and chemical stability.

## 4. Conclusion

Tool life and wear behavior of the cutting tools with AlTiN coating before and after annealing in vacuum and oxygen-containing atmospheres under interrupted cutting operations have been studied in

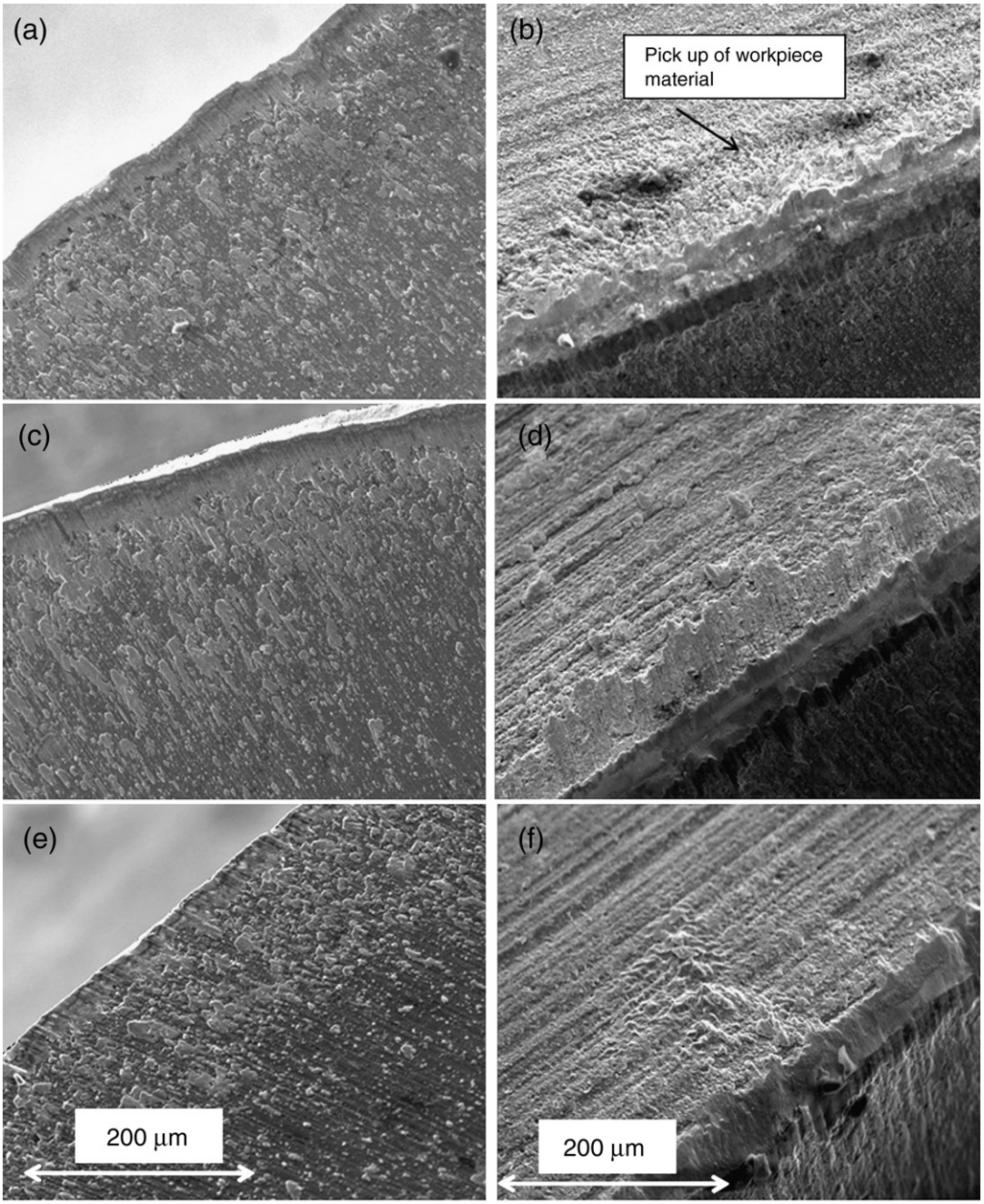


**Fig. 9.** SEM images of the worn surfaces of ball nose end mills: (a) flank surface of the end mill with as-deposited $Al_{67}Ti_{33}N$ film; (b) rake surface of the end mills with as-deposited $Al_{67}Ti_{33}N$ film; (c) flank surface of the end mill with the $Al_{67}Ti_{33}N$ film vacuum annealed at 700 °C; (d) rake surface of the end mill with $Al_{67}Ti_{33}N$ film vacuum annealed at 700 °C; (e) flank surface of the end mill with $Al_{67}Ti_{33}N$ film oxidized at 700 °C; (f) rake surface of the end mill with $Al_{67}Ti_{33}N$ film oxidized at 700 °C.

detail. Advanced characterization techniques such as RBS and XAS show that an outer composite amorphous alumina–titania layer is formed as a result of the post-treatment. However, it was not possible to exclude the possibility of some small amount of ternary Al–Ti–O compounds, or even Al–Ti–O–N compounds, but their relative weight should be low. Cutting tests demonstrated that tool life improvement could be achieved if the annealing of the Al-rich TiAlN coating is performed in the oxygen-containing atmosphere at 700 ºC. Wear behavior of the end mill cutters is improved due to lower sticking of the workpiece material and better chip formation conditions.

## Acknowledgements

This work was partially supported by the Spanish Ministerio de Educación y Ciencia through projects MAT2007-66719-C03-03 and project Consolider CSD2008-00023. Financial support by the Ramón y Cajal Program and Wenner-Gren Foundations is gratefully acknowledged. We also acknowledge beamtime at the 7.0.1 beamline (ALS, Berkeley). We would also like to thank Mr. Jim Garrett (McMaster) for performing of samples annealing in oxygen-containing atmosphere.

## References

[1] H. Holleck, M. Lahres, P. Woll, Surf. Coat. Technol. 41 (1990) 179.
[2] J. Musil, M. Jirout, Surf. Coat. Technol. 201 (2007) 5148.
[3] K.D. Bouzakis, G. Skordaris, S. Hadjiyiannis, I. Mirisidis, N. Michailidis, G. Erkens, I. Wirth, Tribol. Ind. 26 (2004) 3.
[4] J.L. Endrino, G.S. Fox-Rabinovich, C. Gey, Surf. Coat. Technol. 200 (2006) 6840.
[5] A. Hörling, L. Hultman, M. Odén, J. Sjölén, L. Karlsson, Surf. Coat. Technol. 191 (2005) 384.
[6] K. Kutschej, P.H. Mayrhofer, M. Kathrein, P. Polcik, R. Tessadri, C. Mitterer, Surf. Coat. Technol. 200 (2005) 2358.
[7] K. Kutschej, P.H. Mayrhofer, M. Kathrein, P. Polcik, C. Mitterer, Surf. Coat. Technol. 188–189 (2004) 358.
[8] S.M. Lee, H.M. Chow, F.Y. Huang, B.H. Yan, Int. J. Mach. Tools Manufac. 49 (2009) 81.
[9] G.S. Fox-Rabinovich, J.L. Endrino, B.D. Beake, M.H. Aguirre, S.C. Veldhuis, D.T. Quinto, C.E. Bauer, A.I. Kovalev, A. Gray, Surf. Coat. Technol. 202 (2008) 2985.
[10] G.S. Fox-Rabinovich, J.L. Endrino, B.D. Beake, A.I. Kovalev, S.C. Veldhuis, L. Ning, F. Fontaine, A. Gray, Surf. Coat. Technol. 201 (2006) 3524.
[11] K.D. Bouzakis, G. Skordaris, S. Hadjiyiannis, I. Mirisidis, N. Michailidis, PVD film mechanical strength properties and wear behaviour of coated tools after isothermal annealings, Multiscaling in Applied Science and Emerging Technology, Fundamentals and Applications in Mesomechanics, Proceedings of the Sixth International Conference for Mesomechanics, 2004, p. 62.
[12] K.D. Bouzakis, N. Vidakis, N. Michailidis, T. Leyendecker, G. Erkens, G. Fuss, Surf. Coat. Technol. 120–121 (1999) 34.
[13] S. Zhang, D. Sun, Y. Fu, H. Du, Surf. Coat. Technol 198 (2005) 2.
[14] J. Musil, P. Baroch, J. Vlcek, K.H. Nam, J.G. Han, Thin Solid Films 475 (2005) 208.
[15] V. Derflinger, H. Brändle, H. Zimmermann, Surf. Coat. Technol. 113 (1999) 286.
[16] A. Climent-Font, F. Pászti, G. García, M.T. Fernández-Jiménez, F. Agulló, Nucl. Instrum. Methods Phys. Res., B Beam Interact. Mater. Atoms 219–220 (2004) 400.
[17] E. Kótai, Nucl. Instrum. Methods Phys. Res., B Beam Interact. Mater. Atoms 85 (1994) 588.
[18] M. Mayer, SIMNRA User's Guide, 1997.
[19] Y. Liu, H. Wang, J. Yang, B. Huang, Z. Long, J. Mater. Sci. 39 (2004) 4397.
[20] G.S. Fox-Rabinovich, D.S. Wilkinson, S.C. Veldhuis, G.K. Dosbaeva, G.C. Weatherly, Intermetallics 14 (2006) 189.
[21] A. Gutiérrez, M.F. López, J.A. Jiménez, C. Morant, F. Paszti, A. Climent, Surf. Interface Anal. 36 (2004) 977.
[22] A. Gutiérrez, F. Paszti, A. Climent-Font, J.A. Jiménez, M.F. López, J. Mater. Res. 23 (2008) 2245.
[23] M.F. López, L. Soriano, F.J. Palomares, M. Sánchez-Agudo, G.G. Fuentes, A. Gutiérrez, J.A. Jiménez, Surf. Interface Anal. 33 (2002) 570.
[24] L. Soriano, M. Abbate, J.C. Fuggle, C. Jiménez, J.M. Sanz, L. Galán, C. Mythen, H.A. Padmore, Surf. Sci. 281 (1993) 120.
[25] L. Soriano, M. Abbate, H. Pen, M.T. Czyzyk, J.C. Fuggle, J. Electron Spectrosc. Relat. Phenom. 62 (1993) 197.
[26] L. Soriano, M. Abbate, J.C. Fuggle, P. Prieto, C. Jimenez, J.M. Sanz, L. Galan, S. Hofmann, J. Vac. Sci. Technol., A, Films 11 (1993) 47.
[27] A.A. Voevodin, S.V. Prasad, J.S. Zabinski, J. Appl. Physi. 82 (1997) 855.